Proc. Natl. Acad. Sci. USA
Vol. 91, pp. 12458–12462, December 1994
Cell Biology

Source of nuclear calcium signals

NANCY L. ALLBRITTON*†, ELENA OANCEA‡, MICHAEL A. KUHN§, AND TOBIAS MEYER‡

*Department of Neurobiology, Stanford University, Stanford, CA 94305; ‡Department of Cell Biology, Duke University, Durham, NC 27710; and §Molecular Probes, Box 22010, Eugene, OR 97402

Communicated by Lubert Stryer, August 9, 1994

ABSTRACT **Transient increases of Ca^{2+} concentration in the nucleus regulate gene expression and other nuclear processes. We investigated whether nuclear Ca^{2+} signals could be regulated independently of the cytoplasm or were controlled by cytoplasmic Ca^{2+} signals. A fluorescent Ca^{2+} indicator that is targeted to the nucleus was synthesized by coupling a nuclear localization peptide to Calcium Green dextran, a 70-kDa Ca^{2+} indicator. Stimulation of rat basophilic leukemia cells by antigen or by photolytic uncaging of inositol 1,4,5-trisphosphate induced transient increases in nuclear and cytosolic Ca^{2+} concentrations. Elevations in the nuclear Ca^{2+} concentration followed those in the nearby perinuclear cytosol within 200 ms. Heparin-dextran, an inhibitor of the inositol 1,4,5-trisphosphate receptor that is excluded from the nucleus, was synthesized to specifically block the release of Ca^{2+} from cytosolic stores. Addition of this inhibitor suppressed Ca^{2+} transients in the nucleus and the cytosol. We conclude that the Ca^{2+} level in the nucleus is not independently controlled. Rather, nuclear Ca^{2+} increases follow cytosolic Ca^{2+} increases with a short delay most likely due to Ca^{2+} diffusion from the cytosol through the nuclear pores.**

Nuclear Ca^{2+} signals control gene transcription, DNA synthesis, DNA repair, and other nuclear functions (1, 2). In one pathway, gene transcription is induced by Ca^{2+}-mediated activation of nuclear Ca^{2+}/calmodulin-dependent kinase II and by the subsequent phosphorylation of the transcription factors CREB and C/EBPβ (3–5). The mechanism of nuclear Ca^{2+} signaling is not yet known, but an inositol phospholipid signaling system has been identified in the inner membrane of the nuclear envelope (6, 7), and inositol 1,4,5-trisphosphate (IP_3)-gated Ca^{2+} release from isolated nuclei has been observed (8, 9). Nuclear Ca^{2+} concentrations have been reported to be higher than cytosolic ones in sympathetic neurons (10, 11), rat basophilic leukemia cells (RBL cells) (12), and other cells (13, 14) or to be lower in smooth muscle (15) and some neuronal cells (16). These findings suggested that nuclear and cytosolic Ca^{2+} signals are regulated by different mechanisms and can be independent of each other.

In this study, we determined whether nuclear and cytosolic Ca^{2+} signals were independent or coupled. To investigate cytosolic Ca^{2+} signals, we used Calcium Green covalently linked to dextran with a molecular mass of 70 kDa. A fluorescent Ca^{2+} indicator that is targeted to the nucleus was synthesized by addition of a nuclear localization sequence to Calcium Green dextran, termed NuCa-Green. These large molecular size indicators prevent sequestration of the dye into internal organelles and minimize facilitated Ca^{2+} diffusion (17–19). Measurements with these indicators showed that elevations in the nuclear calcium concentration followed those in the nearby cytosol within 200 ms. To determine how nuclear and cytosolic Ca^{2+} signals are coupled, we synthesized an inhibitor of the IP_3 receptor that was excluded from the nucleus. This inhibitor suppressed Ca^{2+} transients in the nucleus and the cytosol. We conclude that the source of nuclear Ca^{2+} signals is cytosolic Ca^{2+} stores and that the nuclear Ca^{2+} concentration is tightly coupled to the cytosolic one by the rapid diffusion of Ca^{2+} from the cytosol into the nucleus.

The publication costs of this article were defrayed in part by page charge payment. This article must therefore be hereby marked "*advertisement*" in accordance with 18 U.S.C. §1734 solely to indicate this fact.

MATERIALS AND METHODS

Preparation of Calcium Green Dextran. Calcium Green dextran (Molecular Probes) had an average dextran molecular mass of 70 kDa and five molecules of Calcium Green per dextran molecule (20). For all experiments, Calcium Green dextran was enriched for large molecular size dextran by ultrafiltration through a membrane with a 100-kDa molecular mass cutoff (Centricon-100; Amicon).

Synthesis and Properties of NuCa-Green. Calcium Green on 70-kDa dextran bearing free amino groups was solubilized at 0.8 mg/ml in 50% (vol/vol) dimethyl sulfoxide/50% (vol/vol) 100 mM Hepes, pH 7. The Calcium Green dextran was reacted with iodoacetic acid *N*-hydroxysuccinimide ester (0.5 mg/ml) and then the nuclear localization sequence peptide CGYGVSRKRPRPG from the polyoma large tumor antigen (165 mg/ml) was added, as described (21). The NuCa-Green was enriched for large molecular size dextran by ultrafiltration through a membrane with a 100-kDa molecular mass cutoff (Centricon-100; Amicon).

The K_d of NuCa-Green for Ca^{2+} was measured using 60 nM NuCa-Green in 100 mM KCl/20 mM Hepes, pH 7.4/50 mM sucrose at 22°C. Portions of this indicator solution received either 10 mM EGTA/10 mM EGTA/10 mM Ca^{2+} or 100 μM Ca^{2+}. An equal volume of these solutions was added to the indicator solution so that the indicator concentration remained constant. The stock 500 mM EGTA/500 mM Ca^{2+} solution was prepared from $CaCO_3$ as described by Tsien and Pozzan (22). Solutions with different free Ca^{2+} concentrations were produced by mixing the indicator solution with 10 mM EGTA and the indicator solution with 10 mM EGTA/10 mM Ca^{2+}. Simultaneously, identical solutions with 2 μM fluo-3 or 2 μM Calcium Green dextran instead of NuCa-Green were also prepared. The fluorescence of the fluo-3 solutions was used to determine the free Ca^{2+} concentration of the buffered Ca^{2+} solutions by using the equation: $[Ca^{2+}] = K_d(F - F_{min})/(F_{max} - F)$, where the K_d of fluo-3 is 316 nM (20). The minimal fluorescence (F_{min}) of the indicator was determined from the solutions with 10 mM EGTA, and the maximal fluorescence (F_{max}) was determined from the solutions with 100 μM Ca^{2+}. To determine the K_d for Ca^{2+} of NuCa-Green and Calcium Green dextran, the fluorescence of the solutions with various free Ca^{2+} concentrations was fitted to the above equation. The K_d of three batches of NuCa-Green was determined and was slightly variable (100, 76, and 69 nM). The K_d of a single batch of Calcium Green dextran

Abbreviations: IP_3, inositol 1,4,5-trisphosphate; BSA-DNP, bovine serum albumin-dinitrophenyl; NuCa-Green, nuclear localization sequence-dextran-Calcium Green.

†Present address: Department of Physiology and Biophysics, University of California, Irvine, CA 92717.

was measured as a control and was 340 nM. This is similar to the reported value of 360 nM (20).

Synthesis of Heparin-Dextran. Heparin-dextran with a molecular mass greater than 70 kDa was synthesized by two techniques: (*i*) Heparin (10 mg/ml) from porcine intestinal mucosa (molecular mass of 13–15 kDa; Calbiochem) was labeled with fluorescein isothiocyanate (10 mg/ml), tetramethylrhodamine isothiocyanate, or an equivalent concentration of dimethyl sulfoxide (20%), as described (23). After addition of glycine (15 mg/ml), the sample was dialyzed (molecular mass cut off, 35 kDa) against 1 liter of water for 20 h at 4°C with eight changes of the dialysis solution. The heparin was dried, resuspended at 50 mg/ml, and reacted with amino-dextran (>75 kDa; 20 mg/ml)/20 mM 1-ethyl-3-(3-dimethylaminopropyl)carbodiimide/5 mM *N*-hydroxysulfosuccinimide, as described (24). Glycine (100 mM) was then added and the reaction mixture was separated on a Sephadex G-75 column. The flow through [determined by Blue dextran (molecular mass = 2000 kDa)] was collected and concentrated by ultrafiltration through a membrane with a 30-kDa molecular mass cutoff (Centriprep-30; Amicon) and then through a membrane with a 100-kDa molecular mass cutoff (Microcon-100; Amicon). The sample was diluted with 5 vol of 130 mM KCl/10 mM KH_2PO_4, pH 7.4 (buffer A), concentrated by ultrafiltration through a membrane with a 100-kDa molecular mass cutoff (Microcon-100; Amicon), then diluted with 10 vol of buffer A, and again concentrated with a Microcon-100. The concentration of heparin was measured with toluidine blue (25). (*ii*) Heparin (67 mg/ml) was activated with cyanogen bromide (13 mg/ml) as described (26) and then separated with a Sephadex G-10 column. Amino-dextran (10 mg/ml) and the derivatized heparin (25 mg/ml) were allowed to react for 15 h. Components of this reaction mixture that were eluted with the void volume on a Sephadex G-75 column were collected and concentrated by ultrafiltration through a membrane with a 10-kDa molecular mass cutoff (Centricon-10; Amicon). This separation and concentration process was repeated, and the concentration of heparin was measured with toluidine blue (25). A portion of this heparin-dextran was fluorescently labeled with an excess of fluorescein isothiocyanate (1000 times the molar concentration of dextran) by incubation at 37°C for 12 h.

Cells. RBL cells (type 2H3) (27), a mast cell tumor line, were incubated with IgE antibody to dinitrophenyl (DNP, 50 μg/ml) at 37°C for 1 h or more, washed five times with 135 mM NaCl/5 mM KCl/10 mM Hepes, pH 7.4/2 mM $MgCl_2$/2 mM $CaCl_2$/10 mM glucose, and then microinjected with the indicators. After 15 min or more at 37°C, the cells were activated by addition of the antigen bovine serum albumin-DNP (BSA-DNP; 5–500 ng/ml).

Measurement of Cellular Fluorescence. To measure changes in the Ca^{2+} concentration in cells, the Ca^{2+} indicators were excited at 488 nm and the fluorescence emission was recorded nonconfocally between 515 and 550 nm on a Nikon inverted microscope with a Noran imaging system. The cytoplasmic fluorescent intensity was always measured 1 μm or more from the nucleus.

Microinjection of Cells. All microinjected probes were dissolved in 130 mM KCl/10 mM KH_2PO_4, pH 7.4, and all injections were made into the cytoplasm of the RBL cells. The concentration of Calcium Green dextran and NuCa-Green in the microinjection pipette was 10–50 mg/ml. When these two indicators were microinjected together, the NuCa-Green concentration was ≈1.5 times greater than the Calcium Green concentration. The brighter fluorescent nuclear signal minimized the contribution of the overlying cytoplasm to the nuclear signal and permitted discrimination of the nuclear area from the cytoplasmic region at all times during measurements.

The concentration of D-*myo*-inositol 1,4,5-trisphosphate $P^{4(5)}$-1-(2-nitrophenyl)ethyl ester (caged IP_3) (Calbiochem) in the microinjection pipette was 0.14 mg/ml. The pipette heparin concentration in the microinjected heparin-dextran was 17.1 mg/ml.

Measurement of the Concentration and Calibration of the Indicators in Cells. To measure the approximate concentration of the Ca^{2+} indicators in cells, the fluorescence intensity of the cells microinjected with the indicators was measured confocally and compared to confocal measurements of the fluorescence intensity of Ca^{2+}-saturated Calcium Green dextran placed between two coverslips. The Ca^{2+} concentration in the unstimulated cells was assumed to be ≈100 nM (12, 28). Thus for NuCa-Green ($K_d \approx 100$ nM), 50% of the indicator was assumed to be bound to Ca^{2+} in unstimulated cells. For Calcium Green dextran ($K_d \approx 360$ nM), 25% of the indicator was assumed to be bound to Ca^{2+} in unstimulated cells. The intracellular concentration of each of the indicators was variable between 4 and 20 μM, corresponding to concentrations of Calcium Green between 20 and 100 μM.

The apparent free Ca^{2+} concentration in cells microinjected solely with NuCa-Green was calibrated with the equation: $[Ca^{2+}] = K_d f/(1 - f)$, where $f = (F - F_{min})/(F_{max} - F_{min})$, $F_{min} = 0.05 F_{max}$, and $K_d = 100$ nM. F_{max} of the nuclear and cytosolic NuCa-Green was determined by addition of A23187 (10 μM) to the cells in the presence of 1 mM extracellular Ca^{2+}. The relation of F_{min} to F_{max} was determined for NuCa-Green by measuring the fluorescence of the indicators in the presence of 10 mM EGTA (F_{min}) or 100 μM Ca^{2+} (F_{max}).

Uncaging of IP_3 in Cells. To rapidly change IP_3 concentrations in cells, D-*myo*-inositol-caged IP_3 was microinjected and the cell was UV-irradiated. The volume illuminated by the UV laser was in the shape of a truncated cone. The laser angle was chosen to produce a beam diameter of ≈1 μm at the focal point. The cells were slightly above the focus of the laser to obtain an average illuminated diameter of <2 μm across the cell. Uncaging was always performed in the cytoplasm far from the nucleus of RBL cells unless specifically stated otherwise. The thickness of RBL cells at the periphery, where the uncaging was performed, was <2 μm.

RESULTS

Localization of Calcium Green Dextran and NuCa-Green in Cells. To investigate nuclear Ca^{2+} signals, we used large molecular size fluorescent Ca^{2+} indicators that prevented sequestration of the dye into internal organelles and minimized facilitated calcium diffusion (17–19). Calcium Green covalently linked to a 70-kDa dextran matrix was largely excluded from the nucleus when microinjected into RBL cells (Fig. 1*A*). Examination by confocal microscopy demonstrated that Calcium Green dextran was not visible in the nucleus in >80% of cells. Therefore, a nuclear Ca^{2+} indicator (NuCa-Green) was synthesized by coupling a peptide derived from the nuclear localization sequence of the polyoma large tumor antigen to Calcium Green dextran. NuCa-Green was concentrated in the nucleus within 5–10 min after microinjection at 37°C (Fig. 1*B*). In most cells, <10% of the NuCa-Green remained in the cytosol. However, a few injected cells had >10% of the NuCa-Green in the cytosol. NuCa-Green also localized to the nucleus of PC12 cells and to the nuclei of developing zebrafish embryos.

Measurement of Nuclear and Cytosolic Ca^{2+} Changes. RBL cells that were microinjected only with NuCa-Green were stimulated by cross-linking IgE receptors with the antigen BSA-DNP. This mast cell secretory stimulus produces Ca^{2+} spikes by activation of phospholipase Cγ and production of IP_3 (29). BSA-DNP at low concentrations induced repetitive Ca^{2+} spikes in the nucleus and cytosol with a spike duration

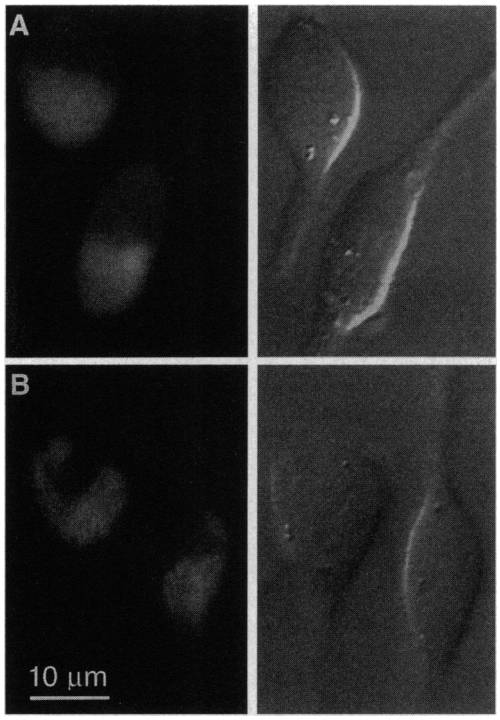

FIG. 1. Properties of the nuclear and cytosolic Ca^{2+} indicators NuCa-Green and Calcium Green dextran. (*A*) Fluorescence image of RBL cells microinjected with Calcium Green dextran, average molecular mass 70 kDa (*Left*) and the corresponding differential interference contrast image (*Right*). (*B*) Fluorescence image of RBL cells microinjected with NuCa-Green (*Left*) and the corresponding differential interference contrast image (*Right*). The final concentrations of NuCa-Green in the nucleus and Calcium Green dextran in the cytosol were variable, 4–20 μM, which corresponded to 20–100 μM Calcium Green.

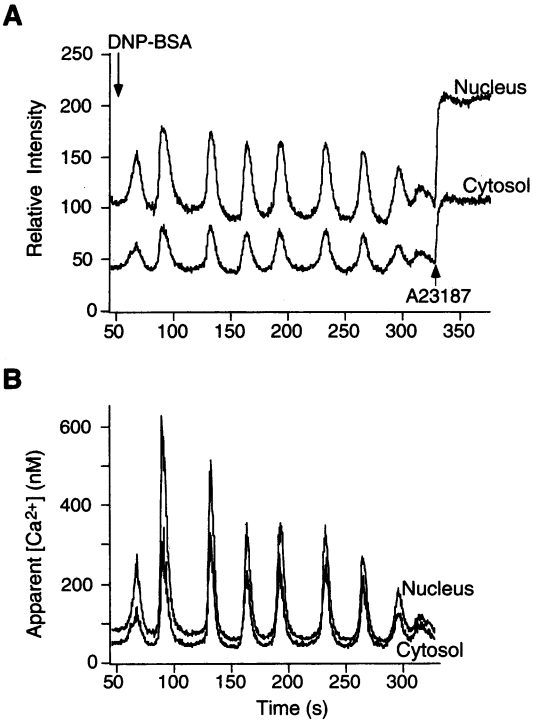

FIG. 2. Nuclear and cytosolic Ca^{2+} responses of RBL cells stimulated with BSA-DNP (5 ng/ml). Cells were microinjected with NuCa-Green only and cytosolic Ca^{2+} responses were measured from a small fraction of the indicator that was not localized to the nucleus. The time resolution was 300 ms. (*A*) Intensity traces from the nucleus and cytosol were plotted on the same intensity scales. (*B*). The trace from *A* was plotted as the calculated Ca^{2+} concentration.

of 5–10 s and interspike intervals of between 20 and 150 s (Fig. 2*A*). Cytosolic and nuclear Ca^{2+} transients always coincided ($n > 30$). Apparent peak Ca^{2+} concentrations in the nucleus appeared to be higher than those in the cytosol when the indicators were calibrated (Fig. 2*B*). Two interpretations are possible: (*i*) IP_3 diffuses into the nucleus and releases Ca^{2+} from nuclear Ca^{2+} stores into the nuclear matrix. This mechanism would allow different nuclear and cytosolic Ca^{2+} levels. (*ii*) Nuclear Ca^{2+} arises by diffusion from the cytosol. RBL cells do not respond to caffeine or ryanodine, and increasing the intracellular Ca^{2+} concentration of permeabilized RBL cells does not cause release of Ca^{2+} from intracellular stores (J. Horne and T.M., unpublished data). Therefore, actual Ca^{2+} levels in the nucleus and cytoplasm would have to be similar but they could appear to be different if the K_d of the Ca^{2+} indicators can be altered by interactions with cytosolic and nuclear components (16, 17, 30–34). For this reason, we analyzed the source of nuclear Ca^{2+} signals by using techniques that did not depend on calibration of the indicators.

Effect of Heparin-Dextran on Cytosolic and Nuclear Ca^{2+} Signals. To determine whether IP_3 releases Ca^{2+} from nuclear Ca^{2+} stores into the nuclear matrix, we synthesized an inhibitor of the IP_3 receptor that was excluded from the nucleus. Because of its large size, heparin-dextran was greatly enriched in the cytoplasm compared to the nucleus, as shown by injection of a fluorescently marked heparin-dextran into RBL cells (Fig. 3*A*). Most cells showed a nearly complete cytosolic localization. Hence, heparin-dextran will predominantly block IP_3 receptors in the cytoplasm but not in the nucleus. Antigen-induced nuclear and cytosolic Ca^{2+} changes were measured in cells that had been injected with heparin-dextran. The expected Ca^{2+} spikes were not observed nor was an increase in cytoplasmic or nuclear Ca^{2+} concentrations ($n = 20$).

Since heparin may inhibit the production of IP_3 by antigen-activated phospholipase C (35), we microinjected RBL cells with caged IP_3. Nuclear and cytoplasmic Ca^{2+} changes were measured after release of IP_3 by a series of pulses of UV radiation of increasing duration. Multiple UV pulses could be applied before the caged IP_3 was consumed. The IP_3 sensitivity of cytosolic and potential nuclear IP_3 receptors in the absence and presence of heparin-dextran was measured (Fig. 3 *B* and *C*). In the absence of heparin-dextran, the Ca^{2+} concentration increased substantially in the nucleus and cytosol of most cells after IP_3 was released by a 30-ms UV pulse (Fig. 3*B*). In contrast, the same amount of IP_3 did not substantially alter the Ca^{2+} concentration in the nucleus or cytosol of most cells loaded with heparin-dextran (Fig. 3*C*). No cell showed a nuclear Ca^{2+} elevation without a corresponding increase in the cytoplasmic Ca^{2+} concentration. Because heparin competitively inhibits IP_3-gated Ca^{2+} release (36), the block by heparin-dextran was not always complete. In 40% of the cells loaded with heparin-dextran, the IP_3 released by a 2-s UV pulse increased the Ca^{2+} concentration in the nucleus and the cytosol. The amount of IP_3 required to overcome the inhibition produced by the cytosolic heparin-dextran was always identical in the nucleus and cytosol. The inhibition of cytosolic receptors for IP_3 increases the concentration of IP_3 required to generate nuclear and cytosolic Ca^{2+} signals. Thus, IP_3 does not release Ca^{2+} from inside the nucleus. The cytosol must be the source of nuclear Ca^{2+} signals.

Measurement of the Delay Time Between Cytosolic and Nuclear Ca^{2+} Increases. To determine how tightly nuclear and cytosolic Ca^{2+} concentrations are coupled, we measured the

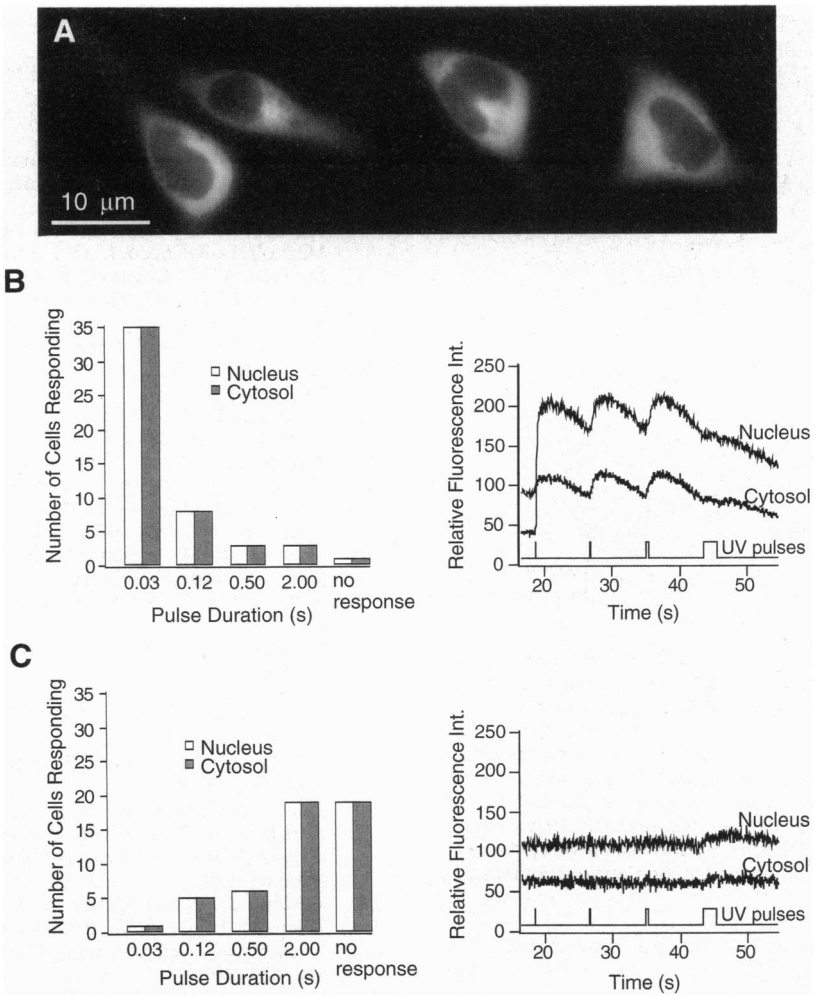

FIG. 3. Effects of heparin-dextran on nuclear and cytosolic Ca^{2+} responses. (*A*) Fluorescent image of RBL cells injected only with fluorescein-labeled heparin-dextran. In this nonconfocal image, the fluorescent intensity of the cytoplasm is more than five times greater than that of the nucleus. (*B*) Histogram of the IP_3 sensitivity of cells without heparin-dextran. RBL cells were injected with the mixture caged IP_3/NuCa-Green/Calcium Green dextran. The cytoplasmic and nuclear fluorescent recording areas were separated by 1–2 μm and were approximately equidistant from the UV beam, which was 2 μm in diameter. A series of UV pulses (30 ms, 125 ms, 500 ms, and 2 s) separated by 8 s was given. The amount of IP_3 released increases with the duration of the pulse; hence, successively higher concentrations of IP_3 are liberated in the cell by this protocol. A cell was said to have responded to the released IP_3 if the fluorescence intensity increased by >20% of the baseline. The lowest concentration of IP_3 or shortest UV pulse to which a cell responded was plotted against the number of cells (*Left*). Responses to the IP_3 released by subsequent longer pulses were not graphed. A typical trace from a cell responding to the IP_3 released by a 30-ms UV pulse is shown (*Right*). Fifty cells were tested for this control experiment. (*C*) RBL cells were injected with the mixture caged IP_3/NuCa-Green/Calcium Green dextran/heparin-dextran. Histogram of the IP_3 sensitivity of cells that contained large molecular size heparin-dextran is shown (*Left*). Most of the 50 recorded cells did not respond to the IP_3 released by maximal UV pulses or responded only to the IP_3 released during the 2-s UV pulse. A trace from a typical nonresponsive cell is shown (*Right*).

delay time between nuclear and cytosolic Ca^{2+} transients. Nuclear and cytosolic Ca^{2+} responses were nearly synchronous when the IP_3 concentration was rapidly increased by local release of caged IP_3 (Fig. 4*A*). When measurements were made at nuclear and perinuclear locations separated by ≈2 μm, <200 ms elapsed between changes in the nuclear and perinuclear Ca^{2+} signals ($n > 10$) (Fig. 4*B*). A schematic drawing shows the respective locations of the recording areas and of the UV-irradiated spot (Fig. 4*C*). An increase in the cytosolic Ca^{2+} concentration was always followed by an increase in the nuclear Ca^{2+} concentration. When the cylinder of the UV beam was placed at other locations within the cell such as pseudopodia or the nucleus, the Ca^{2+} response in the nucleus and in the perinuclear region remained rapid and nearly synchronous. When sufficient Ca^{2+} was released by IP_3 to nearly saturate NuCa-Green ($Ca^{2+} > 300$ nM), the delay time between the fluorescence intensity changes in the nucleus and the cytosol remained the same. Since the nuclear and cytosolic Ca^{2+} signals follow identical kinetic patterns at all observed Ca^{2+} concentrations, the permeability of nuclear pores does not appear to be regulated by Ca^{2+}. In RBL cells, the access of Ca^{2+} signals to the nucleus is not substantially delayed by the nuclear envelope.

DISCUSSION

Two lines of evidence demonstrate that the cytosol is the source of nuclear Ca^{2+} signals in RBL cells. (*i*) Heparin-dextran, which was excluded from the nucleus, blocked elevations in the nuclear Ca^{2+} concentration as efficiently as it blocked those in the cytosol. IP_3 produced in the cytosol does not open Ca^{2+} release channels inside the nucleus. (*ii*) Changes in the nuclear Ca^{2+} concentration followed those in the adjacent cytosol by 200 ms or less at all Ca^{2+} concentrations. In RBL cells, the Ca^{2+} concentration of the nucleus is tightly linked to that of the cytosol. We conclude that nuclear Ca^{2+} signals are produced by diffusion of Ca^{2+} into the nucleus from the cytosol. These results also suggest that

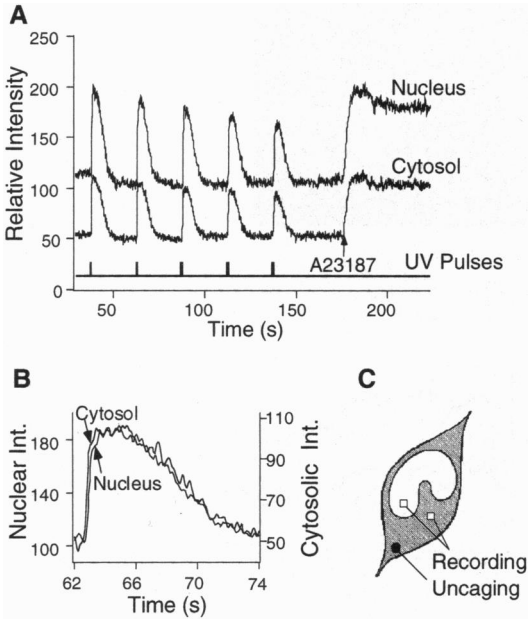

FIG. 4. Delay between nuclear and cytosolic Ca^{2+} responses to pulses of IP_3. (*A*) Fluorescence intensity traces from nuclear and cytosolic locations during multiple UV laser pulses to release IP_3 (five 50-ms pulses). The cells were microinjected with the mixture Calcium Green dextran/NuCa-Green/caged IP_3. The time resolution was 60 ms. (*B*) Expansion of the time scale of the second Ca^{2+} spike in the traces in *A*. The fluorescence intensities of the nuclear and cytosolic traces were normalized so that maximal and minimal intensities are coincident. (*C*) Schematic drawing of the nuclear and cytoplasmic recording sites and of the location of the UV-uncaging spot.

free Ca^{2+} concentrations in the nucleus and perinuclear cytosol are nearly the same for time scales >200 ms. The cytoplasmic origin of nuclear Ca^{2+} ions enables nuclear Ca^{2+} concentrations to be tightly controlled by receptor-mediated production of IP_3 or by the opening of Ca^{2+} channels at the plasma membrane. The fast (<200 ms) transmission of Ca^{2+} signals across the nuclear membrane defines the amplitude of nuclear signals as an average of the Ca^{2+} increases in the perinuclear region and ensures rapid activation of calmodulin and other nuclear Ca^{2+} binding proteins.

We thank L. Stryer, J. Boniface, and others for stimulating discussions and J. Horne and C. Sims for help with several assays used. This work was supported by the David and Lucile Packard Foundation (T.M.), by National Institutes of Health Grant GM48113 (T.M.), by National Institutes of Health Research Fellowship Award 5F32AI0814203 (N.L.A.), and by National Institute of Mental Health Grant MH45324 to L. Stryer.

1. Bachs, O., Agell, N. & Carafoli, E. (1992) *Biochim. Biophys. Acta* **1113,** 259–270.
2. Karin, M. (1992) *FASEB J.* **6,** 2581–2590.
3. Wegner, M., Cao, Z. & Rosenfeld, M. G. (1992) *Science* **256,** 370–373.
4. Sheng, M., McFadden, G. & Greenberg, M. E. (1990) *Neuron* **4,** 571–582.
5. Peunova, N. & Enikolopov, G. (1993) *Nature (London)* **364,** 450–453.
6. Payrastre, B., Nievers, M., Boonstra, J., Breton, M., Verkleij, A. J., VanBergen, E. N. & Henegouwen, P. M. (1992) *J. Biol. Chem.* **267,** 5078–5084.
7. Martelli, A. M., Gilmour, R. S., Bertagnolo, V., Neri, L. M., Manzoli, L. & Cocco, L. (1992) *Nature (London)* **358,** 242–245.
8. Malviya, A. N., Rogue, P. & Vincendon, G. (1990) *Proc. Natl. Acad. Sci. USA* **87,** 9270–9274.
9. Matter, N., Ritz, M., Freyermuth, S., Rogue, P. & Malviya, A. N. (1993) *J. Biol. Chem.* **268,** 732–736.
10. Hernandez-Cruz, A., Sala, F. & Adams, P. R. (1990) *Science* **247,** 858–862.
11. Przywara, D. A., Bhave, S. V., Bhave, A., Wakade, T. D. & Wakade, A. R. (1991) *FASEB J.* **5,** 217–222.
12. Nakato, K., Furuno, T., Inagaki, K., Teshima, R., Terao, T. & Nakanishi, M. (1992) *Eur. J. Biochem.* **209,** 745–749.
13. Birch, B. D., Eng, D. L. & Kocsis, J. D. (1992) *Proc. Natl. Acad. Sci. USA* **89,** 7978–7982.
14. Waybill, M. M., Yelamarty, R. V., Zhang, Y. L., Scaduto, R. C., LaNoue, K. F., Hsu, C. J., Smith, B. C., Tillotson, D. L., Yu, F. T. & Cheung, J. Y. (1991) *Am. J. Physiol.* **261,** E49–E57.
15. Williams. D. A., Becker, P. L. & Fay, F. S. (1987) *Science* **235,** 1644–1648.
16. Al-Mohanna, F. A., Caddy, K. W. T. & Bolsover, S. R. (1994) *Nature (London)* **367,** 745–750.
17. Connor, J. A. (1993) *Cell Calcium* **14,** 185–200.
18. Allbritton, N. L., Meyer, T. & Stryer, L. (1992) *Science* **258,** 1812–1815.
19. Sala, F. & Hernandez-Cruz, A. (1990) *Biophys. J.* **57,** 313–324.
20. Haugland, R. P. (1992) *Molecular Probes Handbook of Fluorescent Probes and Research Chemicals* (Molecular Probes, Eugene, OR).
21. Vincent, J. P. & O'Farrell, P. H. (1992) *Cell* **68,** 923–931.
22. Tsien, R. & Pozzan, T. (1989) *Methods Enzymol.* **172,** 230–262.
23. Nagasawa, K. & Uchiyama, H. (1978) *Biochim. Biophys. Acta* **544,** 430–440.
24. Staros, J. V., Wright, R. W. & Swingle, D. M. (1986) *Anal. Biochem.* **156,** 220–222.
25. Smith, P. K., Mallia, A. K. & Hermanson, G. T. (1980) *Anal. Biochem.* **109,** 466–473.
26. Axen, R., Porath, J. & Ernback, S. (1967) *Nature (London)* **214,** 1302–1304.
27. Metzger, H., Alcaraz, G., Holman, R., Kinet, J. P., Pribluda, V. & Quarto, R. (1986) *Annu. Rev. Immunol.* **4,** 419–470.
28. Millard, P. J., Ryan, T. A., Webb, W. W. & Fewtrell, C. (1989) *J. Biol. Chem.* **264,** 19730–19739.
29. Park, D. J., Min, H. K. & Rhee, S. G. (1991) *J. Biol. Chem.* **266,** 24237–24240.
30. Hove-Madsen, L. & Bers, D. M. (1992) *Biophys. J.* **63,** 89–97.
31. Ross, W. N. (1993) *Biophys. J.* **64,** 1655–1656.
32. Morgan, K. G. (1993) *Biophys. J.* **65,** 561–562.
33. Konishi, M., Olson, A., Hollingworth, S. & Baylor, S. M. (1988) *Biophys. J.* **54,** 1089–1104.
34. Moore, E. D. W., Becker, P. L., Fogarty, K. E., Williams, D. A. & Fay, F. S. (1990) *Cell Calcium* **2/3,** 157–179.
35. Berridge, M. B. (1993) *Nature (London)* **361,** 315–325.
36. Ghosh, T. K., Eis, P. S., Mullaney, J. M., Ebert, C. L. & Gill, D. L. (1988) *J. Biol. Chem.* **263,** 11075–11079.